Indian Journal of Natural Sciences *www.tnsroindia.org.in ©IJONS*

Vol.14 / Issue 81 / Dec / 2023 *International Bimonthly (Print) – Open Access* *ISSN: 0976 – 0997*

RESEARCH ARTICLE

Turkey Femur Bone Derived Hydroxyapatite: an Efficient Catalyst for Toxic Dye Degradation

V.Bhuvaneshwari[1] and S.Sonia[2]*

[1]Research Scholar (Reg. No. 20213042132007), Department of Physics, Holy Cross College (Autonomous), Nagercoil, Kanyakumari District (Affiliated to Manonmaniam Sundaranar University, Tirunelveli) Tamil Nadu, India.
[2]Assistant Professor, Department of Physics, Holy Cross College, (Autonomous), Nagercoil, Kanyakumari District (Affiliated to Manonmaniam Sundaranar University, Tirunelveli), Tamil Nadu, India.

Received: 18 Aug 2023 Revised: 20 Sep 2023 Accepted: 25 Nov 2023

***Address for Correspondence**
S.Sonia
Assistant Professor,
Department of Physics,
Holy Cross College, (Autonomous),
Nagercoil, Kanyakumari District
(Affiliated to Manonmaniam Sundaranar University, Tirunelveli),
Tamil Nadu, India.
E.mail: sonianst@gmail.com

ABSTRACT

Water pollution has emerged as a critical global crisis due to various contaminating factors, especially from textile industries. The release of toxic dyes into water bodies causes significant environmental damage. This study focuses on the extraction of hydroxyapatite from turkey femur bone using a direct calcination process. X-ray diffraction analysis of the extracted HAp confirms the hexagonal structure with space group of P63/m and reveals agglomerated particles averaging 77.3 nm in size via scanning electron microscopy. Elemental analysis validates the presence of calcium, oxygen, and phosphorus elements. Identification of functional groups is analyzed through FTIR analysis. UV-Vis analysis provides valuable insights into absorbance and bandgap values. In terms of practical application, the extracted HAp showcases significant potential as a catalyst in the treatment of wastewater by photocatalytic experiment. Evidently, its efficiency in decomposing congo red and methylene blue dyes is significant, displaying degradation percentages of 90.5% and 99.4% respectively. These findings proved the remarkable catalytic potential of hydroxyapatite derived from femur bones.

Keywords: Turkey bone, Calcination, Optical properties, Waste water treatment, Photocatalysis,

INTRODUCTION

The release of industrial waste from textile industries, paper industries, cosmetics, food beverages, pharmaceutical, and plastic sectors poses a significant threat to the environment due to the presence of vividly colored substances. Colored discharges infused with dyes and entering water systems bring about significant concerns, such as increased chemical oxygen demand (COD), reduced light transmission and hindered proliferation of microorganisms. Artificial dyes exhibit toxicity and carcinogenic properties bring about substantial environmental health issues when exposed. The toxicity of Congo red stems from its conversion into benzidine, a known human carcinogen upon metabolism. Additionally, exposure to this compound has been linked to inducing allergic reactions in individuals. Even at low levels, CR dye significantly disrupts aquatic ecosystems, impacting the delicate balance of the food chain. Additionally, its presence poses health concerns, leading to respiratory issues, diarrhea, and nausea [1]. Methylene blue is considered extremely carcinogenic that has been produced and utilized across various industries for diverse purposes. When ingested, methylene blue poses a significant danger to human health, causing neurological problems and vision damage. Therefore, it's critical to devise advanced approaches capable of eliminating these perilous contaminants from aquatic environments [2].

To tackle this issue, diverse adsorbents such as activated carbons, zeolites and polymers have been utilized to eliminate dye from wastewater. However, their restricted capacity for adsorption, high expenses, and difficulties in separation hinder their widespread application in wastewater treatment. Consequently, there is a demand for an alternative adsorbent that offers high efficacy, cost-effectiveness, safety, ease of production, and regenerative capabilities. Hydroxyapatite ($Ca_{10}(PO_4)_6(OH)_2$) is highly regarded as an important biomaterial due to its outstanding biocompatibility,, bioactivity, ability to promote bone growth, lack of toxicity, non-immunogenic nature. Furthermore, it is recognized as a valuable material for environmental applications because of its unique structure, enabling ionic exchange and effective adsorption of various pollutants [1]. This current research focuses on extracting hydroxyapatite from turkey femur bone via a straightforward calcination process. The objective is to employ this derived substance to degrade detrimental dyes such as congo red and methylene blue, recognized for their harmful effects. To the best of our knowledge, research conducted on utilizing hydroxyapatite derived from femur bones for degradation of toxic dyes is the first time.

EXPERIMENTAL PROCEDURE

Fresh turkey femur bones were obtained from a local market and subjected to pretreatment by boiling in distilled water to eliminate undesired debris like bone marrow and flesh. Following this, they underwent soaking in NaOH to eliminate protein content, followed by chopping, drying in an oven, and calcination at 900°C for a duration of 4 hours [3].

RESULTS AND DISCUSSION

Structural analysis

X-Ray diffraction pattern of Hydroxyapatite calcinated at 900°C within the range of 20-60° is shown in figure 1. The diffraction peaks obtained at 2θ with hkl values are 25.8° (002), 28.1° (102), 28.9° (210), 31.7° (211), 32.1° (112), 32.9° (300), 34° (202), 35.4° (301), 39.2° (212), 39.8° (310), 42° (311), 43.8° (113), 45.3° (203), 46.7° (222), 48.1° (312), 48.6° (320), 49.4° (213), 50.4° (321), 51.2° (410), 52.1° (402), 53.1° (004), 55.8° (322), 57.1° (313). Every peak displayed distinct features of pure HAp, indicating the hexagonal crystalline structure with space group of P63/*m*. the XRD peaks obtained is well matched with the JCPDS pdf no.09-0432. The sharpness of the peaks indicates crystalline nature of the material. Average crystallite size of the sample is calculated using scherrer equation [4].

$\mathbf{D = \frac{K\lambda}{\beta Cos\theta}}$

The percentage of crystallinity and other crystallographic parameters were calculated using the below mentioned formulas and listed in table 1 [5], [6].

Microstrain	$\varepsilon = \beta /4 \tan\theta$
Dislocation density	$\delta = 1/D^2$
Lattice parameters	$1/d^2 = (4/3) \{(h^2 + hk + k^2)/a^2\} + (l^2/c^2)$
Volume	$V = \frac{\sqrt{3}}{2} a^2 . c$
Percent of Crystallinity	$X_c = (A_{cr}/A_{cr}+A_{am}) \times 100\%$

Morphological analysis

The morphology and particle size of the extracted HAp samples were investigated using scanning electron microscopy images shown in figure 2 along with its particle size distribution curve. The SEM analysis reveals a notable characteristic of the HAp sample that, the particles exhibit irregular shapes and tend to be agglomerated. The Image J software is utilized for measuring the average particle size of the HAp material and is calculated to be 77.3nm [7].

Energy dispersive X ray spectroscopy

EDS was utilized to analyze the chemical composition of the extracted HAp material, as depicted in figure 3. The findings revealed that the synthesized HAp particles primarily comprised calcium, phosphorus, and oxygen as their elemental constituents. Notably, hydrogen (H) was absent in the EDX spectra due to the instrument's limitations, which prevent the detection of elements with atomic numbers below five [8]. The signal attributed to carbon (C) originates from the substrate used in the SEM analysis [9]. The Ca/P ratio of the extracted HAp material is found to be 1.66 which is closely related to the stoichiometric HAp.

Fourier transform infrared spectroscopy

The FT-IR spectra offer chemical information regarding the samples, covering a wavelength range spanning from 4000 cm^{-1} to 500 cm^{-1} is shown in figure 4. The identified phosphate bands at 1091 cm^{-1} and 1044 cm^{-1} consistently appear within the 1000–1150 cm^{-1} range, indicative of the $\nu 3$ asymmetric stretching. The peaks seen at 3572 cm^{-1} and 635 cm^{-1} in the spectrum are due to the hydroxyl groups (OH^-) present in commercial HAp, indicating a high level of crystallinity in the HAp structure. The HAp sample exhibits the asymmetric bending of the phosphate group, which is evident at 570 cm^{-1} and 603 cm^{-1} [3].

UV-visible spectroscopy

When a sample is exposed to electromagnetic radiation within the UV/Vis wavelength range, its surface can engage with the incoming radiation through various interactions, including absorption, transmission, and reflection. The UV-Vis absorption spectrum of hydroxyapatite was examined using different wavelengths ranging from 200 to 800 nm, as illustrated in figure 5(a) [10]. HAp particles demonstrate significant absorption in the shorter wavelength spectrum, specifically around 350-400 nanometers. The energy needed to elevate an electron from the valence band to the conduction band is referred to as the band gap energy (Eg). Tauc plots serve as a method to ascertain the bandgap energy.

$\mathbf{\alpha h\upsilon = A [h\upsilon - E_g]^n}$

Where, α is the absorbance coefficient, Eg is the optical bandgap energy of the material, $h\upsilon$ is the photon energy and n is either 2 for direct band gap or 1/2 for indirect band gap. When plotting $h\upsilon$ against $(\alpha h\upsilon)^2$ for n=direct bandgap, the resulting graph helps determine the optical band gap (Eg) which is found to be 3.18 eV [11].

PHOTOCATALYTIC ACTIVITY

Photocatalytic dye degradation initiates with a support material infused with a catalyst exposed to specific light wavelengths, often UV or visible light, matching the catalyst's light absorption. When light interacts with the catalyst, it prompts the creation of electron-hole pairs. These pairs interact with oxygen, water, or hydroxyl ions on the catalyst's surface, generating potent radicals like hydroxyl radicals. These radicals efficiently break down dye molecules located on the catalyst or in the solution. Gradually, this breakdown transforms dye compounds into smaller, less harmful substances, ultimately converting them into harmless byproducts, such as water, carbon dioxide, and mineral salts. Optimizing the efficiency of this photocatalytic process involves monitoring factors like catalyst concentration, light intensity, and duration. Utilizing natural bone-derived hydroxyapatite as a support material, this eco-friendly approach exhibits substantial potential for treating dye contaminated wastewater without producing detrimental residues [12].

Photocatalytic experiment

A concentrated solution, comprising 2 ppm of congo red (CR) and methylene blue (MB) dyes at a concentration of 1000 mg per liter, was formulated using distilled water. To carry out the batch experiments, 100 ml of this dye solution was utilized in 200 ml flasks with various known concentrations. Each flask was supplemented with 5 mg (0.005g) of adsorbent. Subsequently, UV light exposure initiated a photochemical reaction. Sampling at regular intervals and utilizing a UV-Vis spectrophotometer for absorbance measurement assisted in monitoring the pollutant concentration in the solution during the photocatalytic degradation process. The degradation percentage was determined by employing the following formula [12].

Degradation efficiency (%) = A_0-A_t /A_0 x 100

Where, A_0 is the initial absorbance of the dye, A_t is the absorbance at time t after degradation of dye. The process involves Hydroxyapatite as a catalyst for the photocatalytic degradation of congo red and methylene blue dye under UV light. The maximum absorption wavelength of congo red and methylene blue dye is 499nm and 663nm. Figure 7 illustrates the degradation of dye solutions in approximately 50 minutes for congo red dye and 20 minutes for methylene blue dye when HAp was employed as a catalyst. The flat line of the absorption curve indicates the complete degradation of toxic dyes from the water solution as shown in figure 6. The calculated degradation percentage is found to be 90.5% for congo red and 99.4% for methylene blue dye. The photocatalytic degradation curve and efficiency is shown in figure 8 & 9.

CONCLUSION

This study has successfully demonstrated the extraction of hydroxyapatite from turkey femur bones utilizing a simple calcination process. Characterization techniques confirmed the purity of phase and functional properties of the HAp. The findings demonstrate that the femur bone derived hydroxyapatite as an effective catalyst for the degradation of congo red and methylene blue dyes present in industrial wastewater. These results highlight the promising application of this biomaterial in addressing environmental challenges posed by textile industry pollutants. Further research could explore optimization strategies for enhancing the efficiency and scalability of this extraction process, paving the way for its practical implementation in large scale environmental remediation efforts.

ACKNOWLEDGEMENT

I acknowledge Dr. S. Sonia for her valuable guidance.

REFERENCES

1. C. Srilakshmi and R. Saraf, "Ag-doped hydroxyapatite as efficient adsorbent for removal of Congo red dye from aqueous solution: Synthesis, kinetic and equilibrium adsorption isotherm analysis," *Microporous Mesoporous Mater.*, vol. 219, no. October 2020, pp. 134–144, 2016, doi: 10.1016/j.micromeso.2015.08.003.
2. M. I. Din, R. Khalid, J. Najeeb, and Z. Hussain, "Fundamentals and photocatalysis of methylene blue dye using various nanocatalytic assemblies- a critical review," *J. Clean. Prod.*, vol. 298, p. 126567, 2021, doi: 10.1016/j.jclepro.2021.126567.
3. A. Esmaeilkhanian, F. Sharifianjazi, A. Abouchenari, A. Rouhani, N. Parvin, and M. Irani, "Synthesis and Characterization of Natural Nano-hydroxyapatite Derived from Turkey Femur-Bone Waste," *Appl. Biochem. Biotechnol.*, vol. 189, no. 3, pp. 919–932, 2019, doi: 10.1007/s12010-019-03046-6.
4. M. K. Herliansyah, D. A. Nasution, M. H. Bin Abdul Shukor, A. Ide-Ektessabi, M. W. Wildan, and A. E. Tontowi, "Preparation and Characterization of Natural Hydroxyapatite: A Comparative Study of Bovine Bone Hydroxyapatite and Hydroxyapatite from Calcite," *Mater. Sci. Forum*, vol. 561–565, pp. 1441–1444, 2007, doi: 10.4028/www.scientific.net/msf.561-565.1441.
5. P. S. K. Senthilarasan, "Synthesis and Characterization of Hydroxyapatite with Gum Arabic (Biopolymer) Nano Composites for Bone Repair," *Int. J. Sci. Res.*, vol. 3, no. 11, p. —, 2014, [Online]. Available: https://www.ijsr.net/archive/v3i11/T0NUMTQxNjI1.pdf
6. M. A. Nawaz *et al.*, "Microstructural study of as grown and 650 °C annealed ZnO nanorods: X-ray peak profile analysis," *Dig. J. Nanomater. Biostructures*, vol. 11, no. 2, pp. 537–546, 2016.
7. H. Hamidah, Iriany, and M. Zuqni, "Characterization of hydroxyapatite from chicken bone via precipitation," *Key Eng. Mater.*, vol. 744 744 KE, pp. 485–489, 2017, doi: 10.4028/www.scientific.net/KEM.744.485.
8. S. Sebastiammal *et al.*, "Synthesis, Characterization, Antibacterial, Antifungal, Antioxidant, and Anticancer Activities of Nickel-Doped Hydroxyapatite Nanoparticles," *Fermentation*, vol. 8, no. 12, 2022, doi: 10.3390/fermentation8120677.
9. H. S. Ragab, F. A. Ibrahim, F. Abdallah, A. A. Al-Ghamdi, F. El-Tantawy, and F. Yakuphanoglu, "Synthesis and In Vitro Antibacterial Properties of Hydroxyapatite Nanoparticles," *IOSR J. Pharm. Biol. Sci.*, vol. 9, no. 1, pp. 77–85, 2014, doi: 10.9790/3008-09167785.
10. F. Y. Rajhi, I. S. Yahia, H. Y. Zahran, and M. Kilany, "Synthesis, structural, optical, dielectric properties, gamma radiation attenuation, and antimicrobial activity of V-doped hydroxyapatite nanorods," *Mater. Today Commun.*, vol. 26, no. June 2020, p. 101981, 2021, doi: 10.1016/j.mtcomm.2020.101981.
11. P. Raizda, S. Gautam, B. Priya, and P. Singh, "Preparation and photocatalytic activity of hydroxyapatite supported BiOCl nanocomposite for oxytetracyline removal," *Adv. Mater. Lett.*, vol. 7, no. 4, pp. 312–318, 2016, doi: 10.5185/amlett.2016.5847.
12. Y. Yang *et al.*, "Chitosan-capped ternary metal selenide nanocatalysts for efficient degradation of Congo red dye in sunlight irradiation," *Int. J. Biol. Macromol.*, vol. 167, no. September, pp. 169–181, 2021, doi: 10.1016/j.ijbiomac.2020.11.167.

Table 1: Crystallographic parameters of Hydroxyapatite

Samples	Crystallite size(D) nm	Strain(ε)	Dislocation density (δ) x10^{14} (lines/m^2)	Lattice Parameters(Å)	Volume (V) (Å)^3	Crystallinity (%)
Hydroxyapatite	43.1	0.00249	5.38	a=b=9.412 c=6.883	528	96.1%

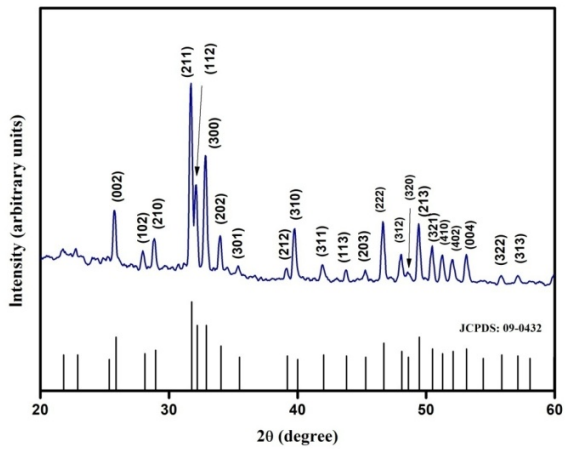

Figure 1: X-ray diffraction pattern of Hydroxyapatite from femur bone of turkey

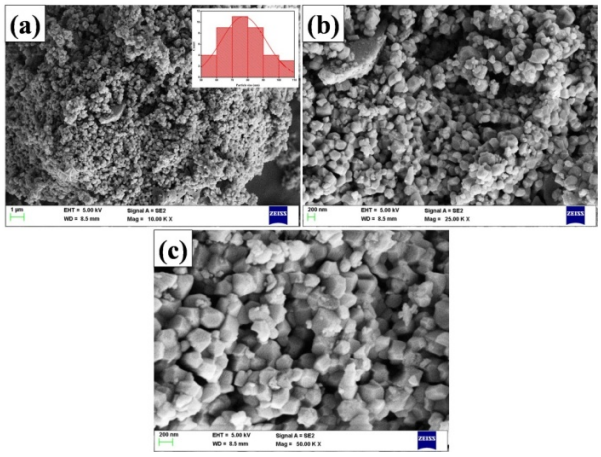

Figure 2: (a-c) Scanning electron microscopy images of Hydroxyapatite in different magnifications with particle size distribution curve

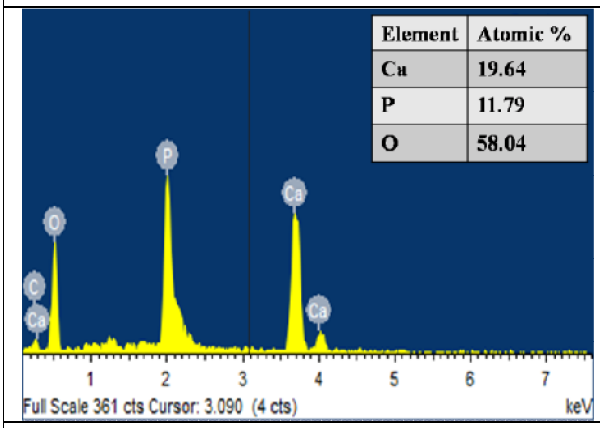

Figure 3: Elemental composition of Hydroxyapatite

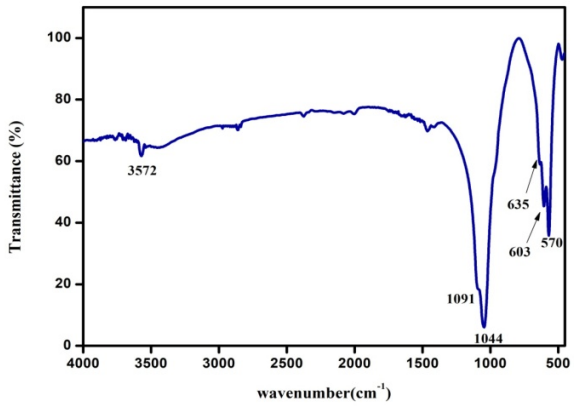

Figure 4: Fourier transform infrared spectroscopy of Hydroxyapatite

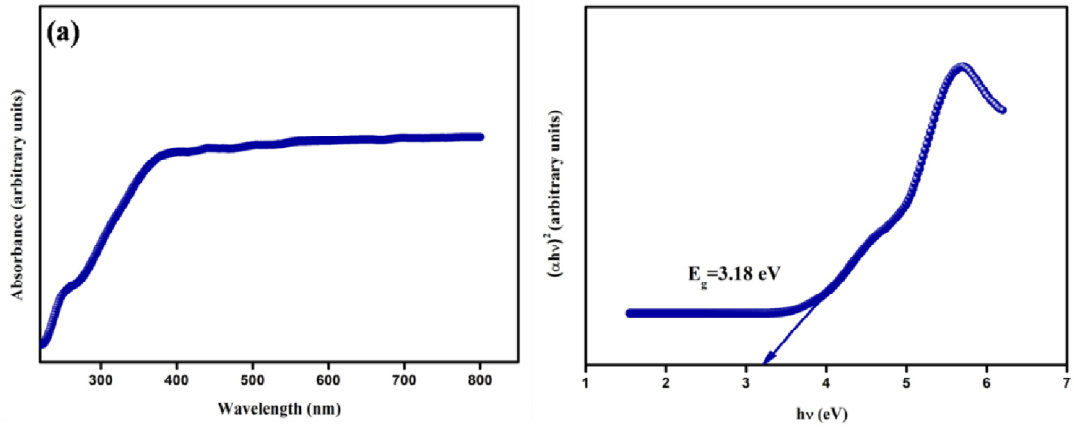

Figure 5: (a) UV-visible absorption spectra (b) tauc plot of Hydroxyapatite

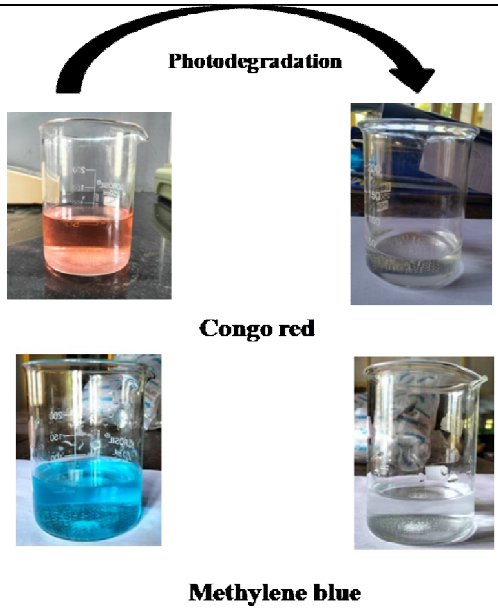

Figure 6: Photocatalytic degradation of Congo red and methylene blue dye solution

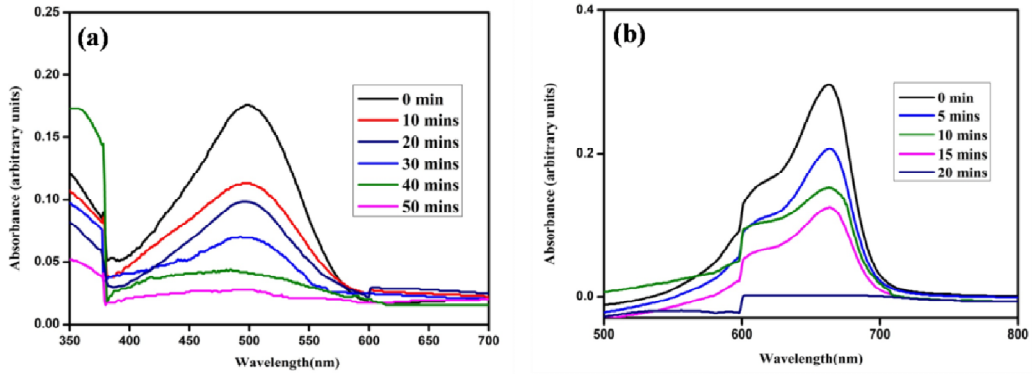

Figure 7: Photodegradation absorption spectra obtained for (a) Congo red (b) Methylene blue

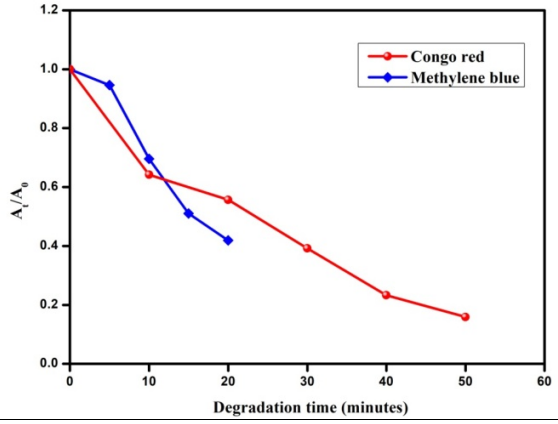

Figure 8: Photocatalytic degradation curve of Congo red and methylene blue dyes

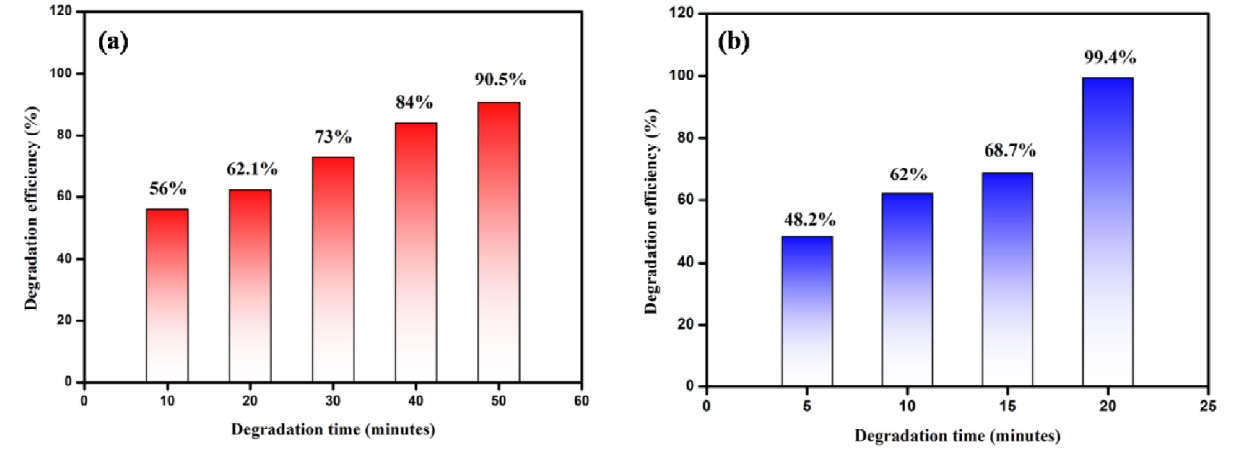

Figure 9: Degradation efficiency of Congo red and methylene blue dyes